

PREPARATION AND OPERATIONS OF THE MISSION PERFORMANCE
CENTRE (MPC) FOR THE COPERNICUS SENTINEL-3 MISSION

S3-A SLSTR Cyclic Performance Report

Cycle No. 024

Start date: 27/10/2017

End date: 23/11/2017



*Mission
Performance
Centre*



Ref.: S3MPC.RAL.PR.02-024
Issue: 1.0
Date: 30/11/2017
Contract: 4000111836/14/I-LG

Customer: ESA	Document Ref.: S3MPC.RAL.PR.02-024
Contract No.: 4000111836/14/I-LG	Date: 30/11/2017
	Issue: 1.0

Project:	PREPARATION AND OPERATIONS OF THE MISSION PERFORMANCE CENTRE (MPC) FOR THE COPERNICUS SENTINEL-3 MISSION		
Title:	S3-A SLSTR Cyclic Performance Report		
Author(s):	SLSTR ESLs		
Approved by:	D. Smith, SLSTR ESL Coordinator	Authorized by	Frédéric Rouffi, OPT Technical Performance Manager
Distribution:	ESA, EUMETSAT, S3MPC consortium		
Accepted by ESA	S. Dransfeld, MPC Deputy TO for OPT P. Féménias, MPC TO		
Filename	S3MPC.RAL.PR.02-024 - i1r0 - SLSTR Cyclic Report 024.docx		

Disclaimer

The work performed in the frame of this contract is carried out with funding by the European Union. The views expressed herein can in no way be taken to reflect the official opinion of either the European Union or the European Space Agency.





Table of content

1	INSTRUMENT MONITORING	1
1.1	INSTRUMENT TEMPERATURES.....	1
1.2	SCANNER PERFORMANCE	5
1.3	DETECTOR NOISE LEVELS	7
1.3.1	<i>VIS and SWIR channel signal-to-noise.....</i>	<i>7</i>
1.3.2	<i>TIR channel NEDT.....</i>	<i>9</i>
1.4	CALIBRATION FACTORS	11
1.4.1	<i>VIS and SWIR VISCAL signal response.....</i>	<i>11</i>
2	LEVEL-1 PRODUCT VALIDATION	13
2.1	GEOMETRIC CALIBRATION/VALIDATION	13
2.2	RADIOMETRIC VALIDATION	14
2.3	IMAGE QUALITY	14
3	LEVEL 2 SST VALIDATION	15
3.1	DEPENDENCE ON LATITUDE, TCWV, SATELLITE ZA AND DATE	15
3.2	SPATIAL DISTRIBUTION OF MATCH-UPS.....	16
3.3	MATCH-UPS STATISTICS	17
4	LEVEL 2 LST VALIDATION.....	18
4.1	CATEGORY-A VALIDATION	18
4.2	CATEGORY-C VALIDATION	20
5	EVENTS	21
6	APPENDIX A	22

	<p>Sentinel-3 MPC</p> <p>S3-A SLSTR Cyclic Performance Report</p> <p>Cycle No. 024</p>	<p>Ref.: S3MPC.RAL.PR.02-024</p> <p>Issue: 1.0</p> <p>Date: 30/11/2017</p> <p>Page: v</p>
--	---	---

List of Figures

Figure 1: Detector temperatures for each channel from 1st March 2016. Discontinuities occur for the infrared channels where the FPA was heated for decontamination or following an anomaly. The vertical dashed lines indicate the start and end of each cycle. Each dot represents the average temperature in one orbit. ----- 1

Figure 2: Blackbody temperature and baseplate gradient trends. The vertical dashed lines indicate the start and end of each cycle. Each dot represents the average temperature in one orbit. ----- 2

Figure 3: Baffle temperature trends. The vertical dashed lines indicate the start and end of each cycle. Each dot represents the average temperature in one orbit.----- 3

Figure 4: Opto-Mechanical Enclosure (OME) temperature trends showing the paraboloid stops and flip baffle (top two plots) and optical bench and scanner and flip assembly (lower two plots). The top two plots only show data starting from 30th July 2016. The vertical dashed lines indicate the start and end of each cycle. Each dot represents the average temperature in one orbit. ----- 4

Figure 5: Scanner and flip jitter, showing mean, stddev and max/min position per orbit compared to the expected one for the nadir view. The vertical dashed lines indicate the start and end of each cycle. ----- 5

Figure 6: Scanner and flip jitter, showing mean, stddev and max/min position per orbit compared to the expected one for the oblique view. The vertical dashed lines indicate the start and end of each cycle. --- 6

Figure 7: VIS and SWIR channel signal-to-noise of the measured VISCAL signal in each orbit. Different colours indicate different detectors.----- 8

Figure 8: NEDT trend for the thermal channels. Blue points were calculated from the cold blackbody signal and red points from the hot blackbody. Horizontal lines indicate the requirement (dashed) and goal (dotted) as well as the measured values on ground (red and blue dashed). ----- 9

Figure 9: VISCAL signal trend for VIS channels (nadir view). -----11

Figure 10: VISCAL signal trend for SWIR channels (nadir view).-----12

Figure 11: Daily offset results in km from the GeoCal Tool analysis for Nadir along and across track (top two plots) and Oblique along and across track (bottom two plots). The error bars show the standard deviation. The x-axis shows the date (month/year).-----13

Figure 12: Daytime Level-3 image for visible channels on 2nd November 2017. -----14

Figure 13: Dependence of median and robust standard deviation of match-ups between SLSTR SST_{skin} and drifting buoy SST_{depth} for Cycle 24 as a function of latitude, total column water vapour (TCWV), satellite zenith angle and date. The data gap towards the end of the cycle is due to a delay in match-up production.-----15

Figure 14: Spatial distribution of match-ups between SLSTR SST_{skin} and drifting buoy SST_{depth} for Cycle 24.16

Figure 15: Validation of the SL_2_LST product over the mid-July to mid-November reprocessed period at three Gold Standard in situ stations managed by the Karlsruhe Institute of Technology: Evora, Portugal (left); Gobabeb, Namibia (centre); Kalahari-Heimat, Namibia (right). [Results courtesy of Maria Martin through the GlobTemperature Project]-----18

Figure 16: Validation of the SL_2_LST product over the mid-July to mid-November reprocessed period at the seven Gold Standard in situ stations of the SURFRAD network plus a Gold Standard station from the ARM network: Bondville, Illinois top-(left); Desert Rock, Nevada (top-centre); Fort Peck, Montana (top-right); Goodwin Creek, Mississippi (middle-left); Penn State University, Pennsylvania (middle-centre); Sioux Fall, South Dakota (middle-right); Table Mountain, Colorado (bottom-left); and Southern Great Plains, Oklahoma (bottom-centre). -----19

Figure 17: Examples of granules affected by the loss of data on 14th November (12:17-12:20 on the left and 12:40-12:43 on the right). -----21

List of Tables

Table 1: Average reflectance factor, and signal-to-noise ratio of the measured VISCAL signal for cycles 013-024, averaged over all detectors for the nadir view. ----- 7

Table 2: Average reflectance factor, and signal-to-noise ratio of the measured VISCAL signal for cycles 013-024, averaged over all detectors for the oblique view. ----- 7

Table 3: NEDT for cycles 013-024 averaged over all detectors for both Earth views towards the +YBB (hot).-----10

Table 4: NEDT for cycles 013-024 averaged over all detectors for both Earth views towards the -YBB (cold).-----10

Table 5: SLSTR drifter match-up statistics for Cycle 24. -----17



1 Instrument monitoring

1.1 Instrument temperatures

- ❖ Instrument temperatures were stable and consistent with expected values following the decontamination phase which was performed towards the end of Cycle 20.
- ❖ In Cycle 24, blackbody, baffle and OME temperatures were rising as the Earth approaches perihelion, but are still within expected ranges. The temperatures will be monitored carefully in the coming weeks to make sure the +Y blackbody stays below 305K which is the limit for accurate calibration of S7. Gradients across the blackbody baseplate are stable and within their expected range.

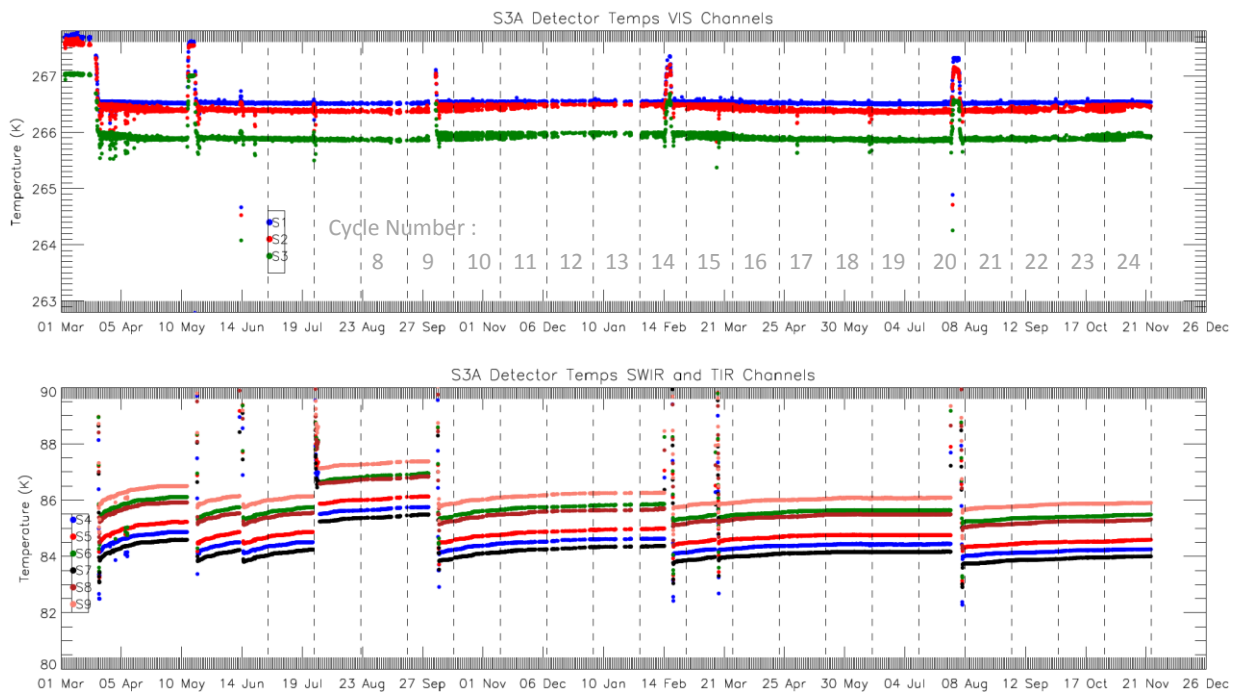


Figure 1: Detector temperatures for each channel from 1st March 2016. Discontinuities occur for the infrared channels where the FPA was heated for decontamination or following an anomaly. The vertical dashed lines indicate the start and end of each cycle. Each dot represents the average temperature in one orbit.



Sentinel-3 MPC
S3-A SLSTR Cyclic Performance Report
Cycle No. 024

Ref.: S3MPC.RAL.PR.02-024
Issue: 1.0
Date: 30/11/2017
Page: 2

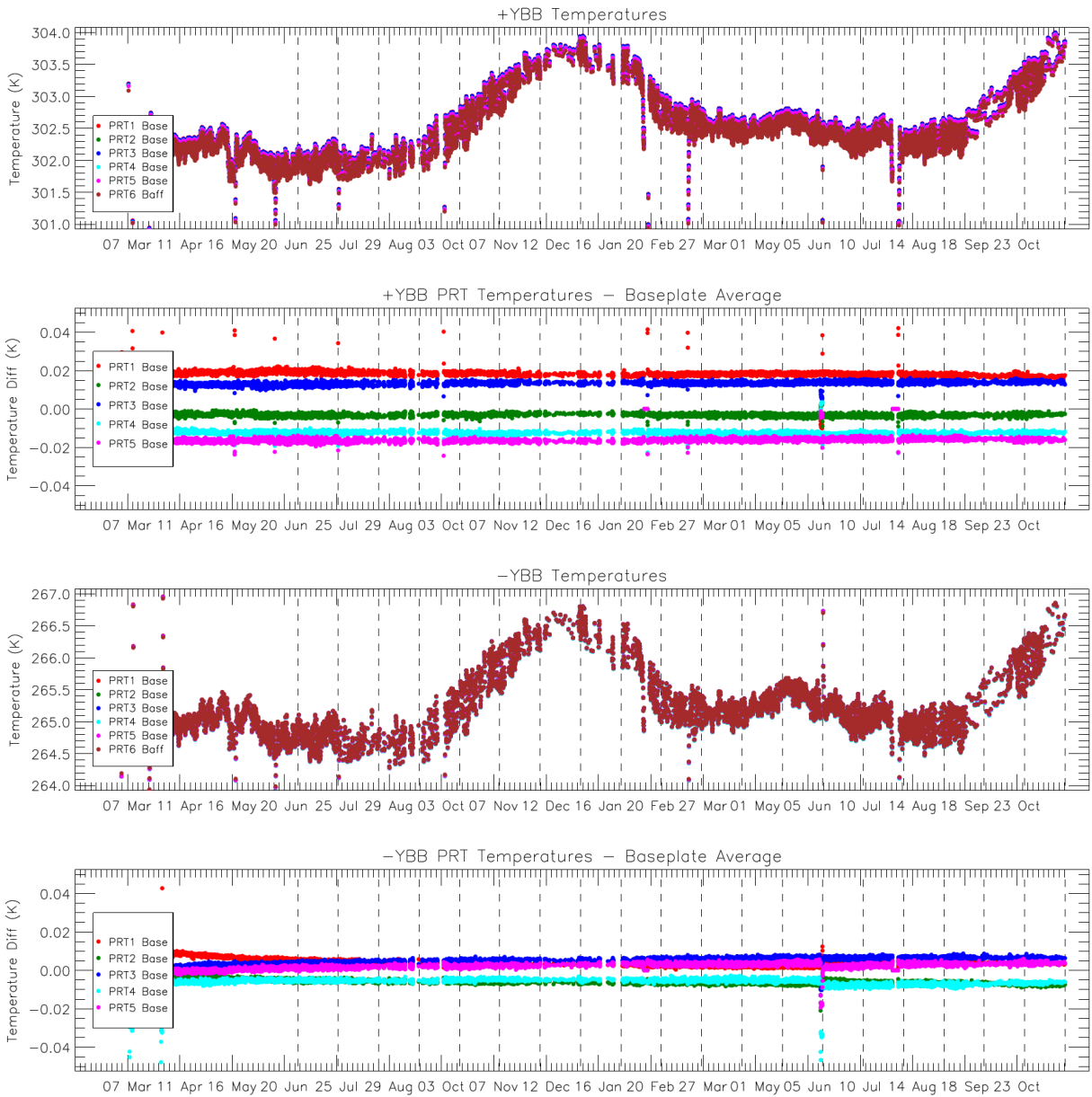


Figure 2: Blackbody temperature and baseplate gradient trends. The vertical dashed lines indicate the start and end of each cycle. Each dot represents the average temperature in one orbit.

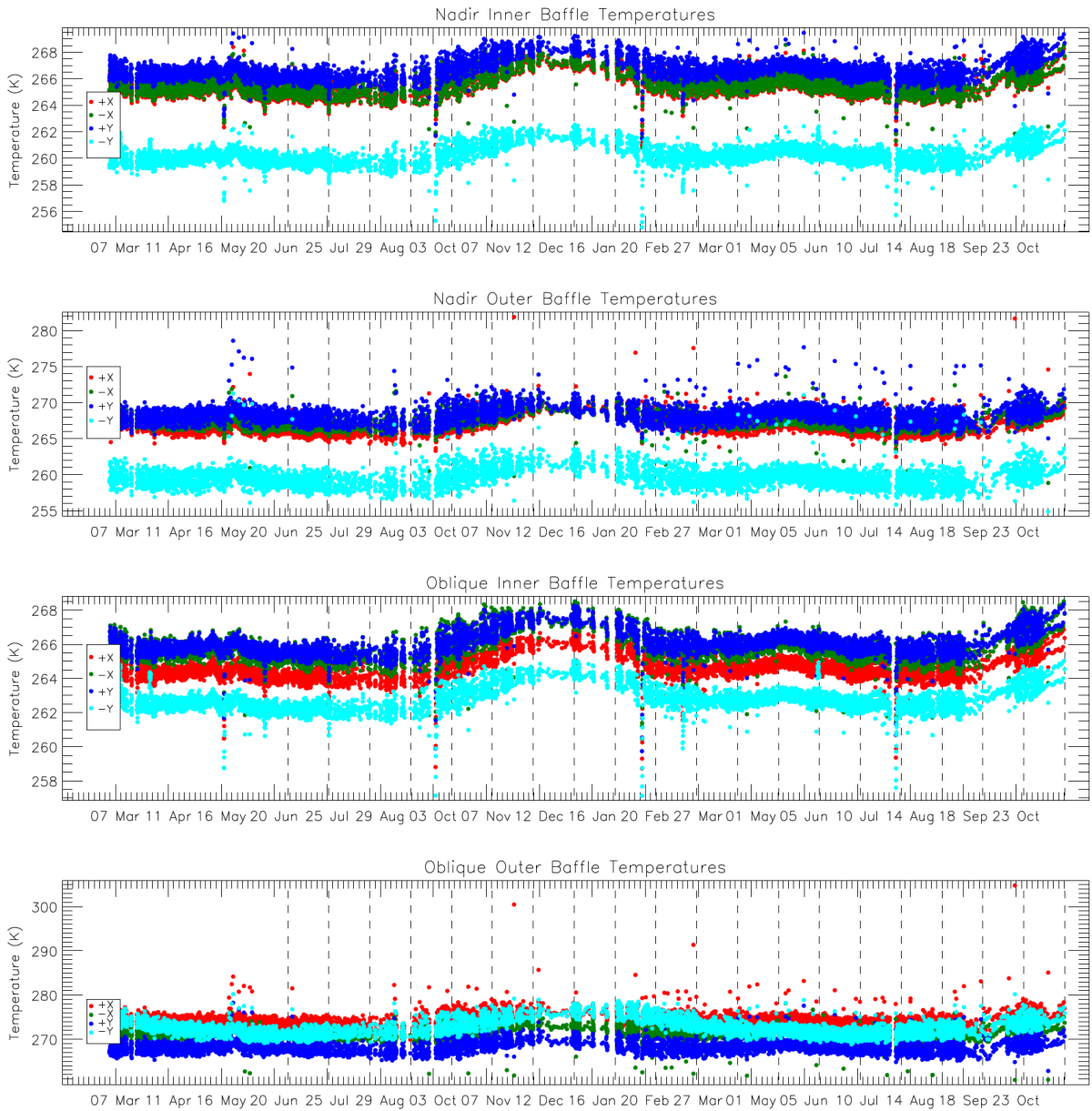


Figure 3: Baffle temperature trends. The vertical dashed lines indicate the start and end of each cycle. Each dot represents the average temperature in one orbit.



Sentinel-3 MPC
S3-A SLSTR Cyclic Performance Report
Cycle No. 024

Ref.: S3MPC.RAL.PR.02-024
Issue: 1.0
Date: 30/11/2017
Page: 4

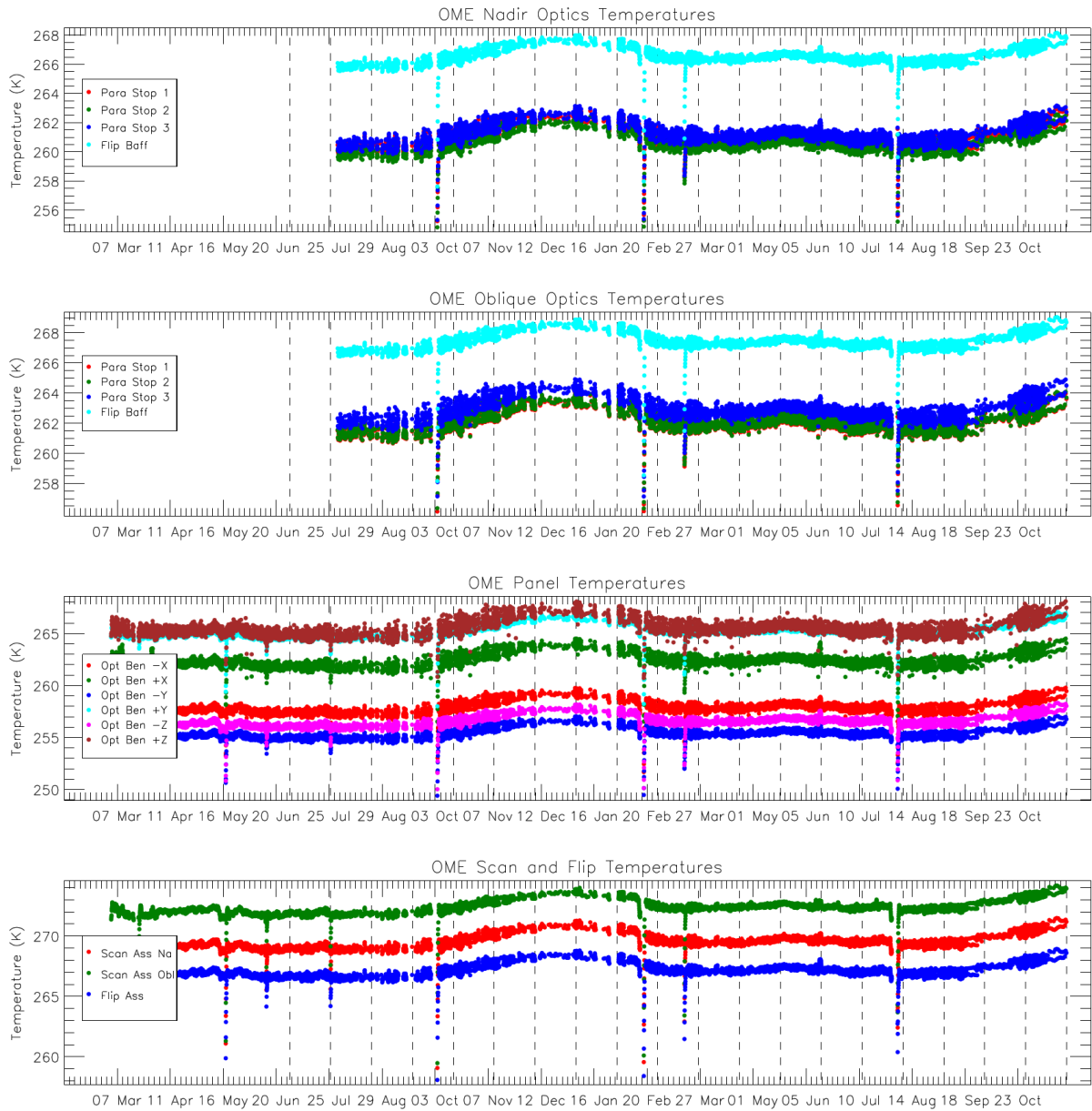


Figure 4: Opto-Mechanical Enclosure (OME) temperature trends showing the paraboloid stops and flip baffle (top two plots) and optical bench and scanner and flip assembly (lower two plots). The top two plots only show data starting from 30th July 2016. The vertical dashed lines indicate the start and end of each cycle. Each dot represents the average temperature in one orbit.



1.2 Scanner performance

Scanner performance has been consistent with previous operations and within required limits.

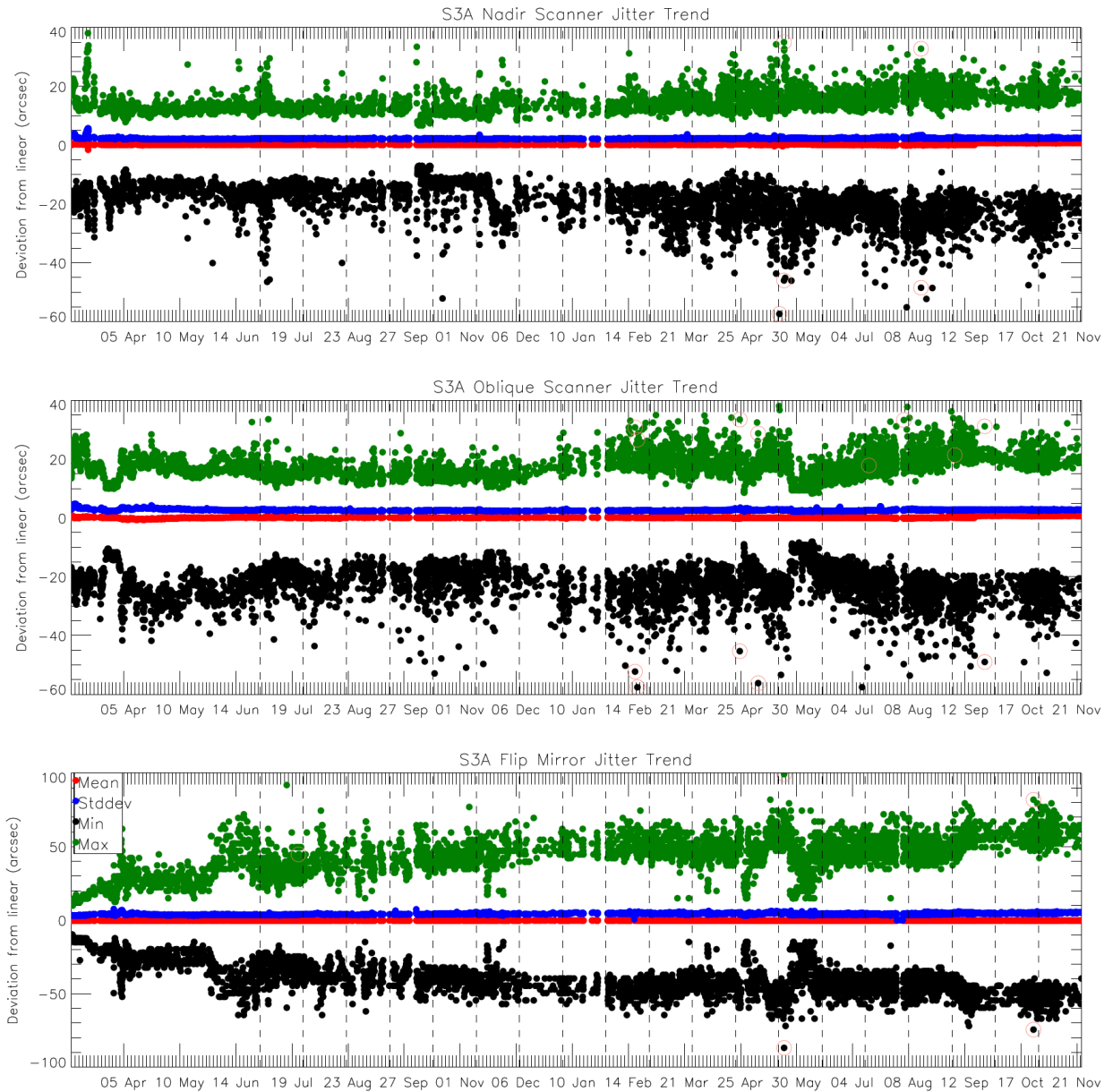


Figure 5: Scanner and flip jitter, showing mean, stddev and max/min position per orbit compared to the expected one for the nadir view. The vertical dashed lines indicate the start and end of each cycle.

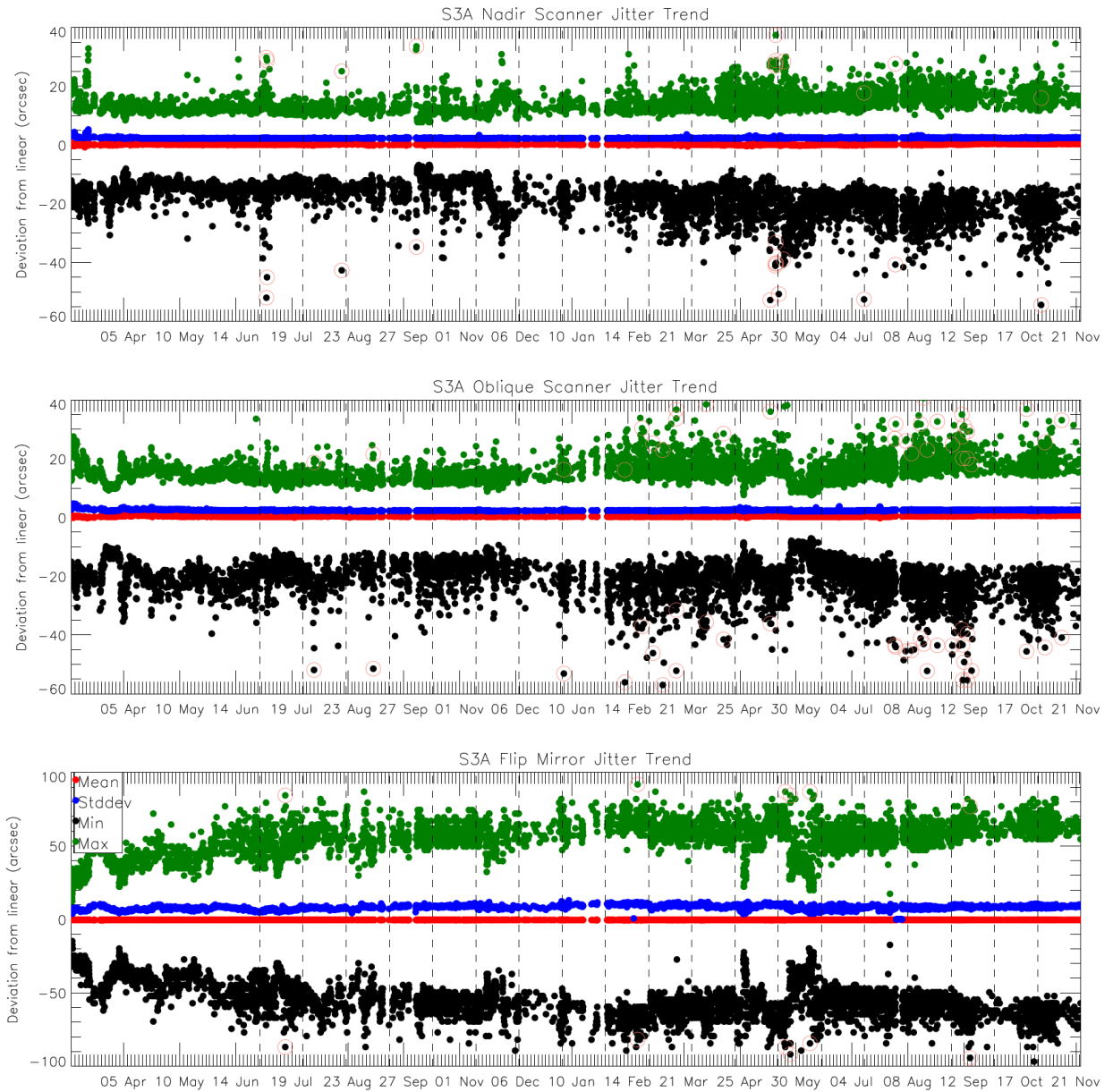


Figure 6: Scanner and flip jitter, showing mean, stddev and max/min position per orbit compared to the expected one for the oblique view. The vertical dashed lines indicate the start and end of each cycle.



1.3 Detector noise levels

1.3.1 VIS and SWIR channel signal-to-noise

The VIS and SWIR channel noise was stable and consistent with previous operations - the signal-to-noise ratio of the measured VISCAL signal is plotted in Figure 7. Table 1 and Table 2 give the average signal-to-noise in each cycle (excluding the anomaly/decontamination period in Cycle 20). Note that this averages over the significant detector-detector dispersion for the SWIR channels that is shown in Figure 7.

Table 1: Average reflectance factor, and signal-to-noise ratio of the measured VISCAL signal for cycles 013-024, averaged over all detectors for the nadir view.

	Average Reflectance Factor	Nadir Signal-to-noise ratio											
		Cycle 013	Cycle 014	Cycle 015	Cycle 016	Cycle 017	Cycle 018	Cycle 019	Cycle 020	Cycle 021	Cycle 022	Cycle 023	Cycle 024
S1	0.187	226	217	224	233	234	231	229	233	231	231	234	237
S2	0.194	234	227	230	236	236	232	231	235	235	234	239	235
S3	0.190	230	221	230	236	238	228	231	230	229	228	234	230
S4	0.191	139	137	139	142	140	140	139	137	135	135	138	240
S5	0.193	234	234	233	233	235	236	233	232	232	230	235	236
S6	0.175	143	141	144	142	143	143	142	140	136	139	142	145

Table 2: Average reflectance factor, and signal-to-noise ratio of the measured VISCAL signal for cycles 013-024, averaged over all detectors for the oblique view.

	Average Reflectance Factor	Oblique Signal-to-noise ratio											
		Cycle 013	Cycle 014	Cycle 015	Cycle 016	Cycle 017	Cycle 018	Cycle 019	Cycle 020	Cycle 021	Cycle 022	Cycle 023	Cycle 024
S1	0.166	238	229	236	243	247	246	242	241	241	243	243	248
S2	0.170	241	232	241	248	251	249	247	247	244	244	253	250
S3	0.168	237	227	236	245	249	244	242	239	234	240	247	240
S4	0.166	108	107	108	108	111	110	109	108	108	108	110	111
S5	0.166	169	169	172	169	169	171	168	168	168	168	172	172
S6	0.155	105	106	107	109	109	110	108	106	108	107	111	109



Sentinel-3 MPC

S3-A SLSTR Cyclic Performance Report

Cycle No. 024

Ref.: S3MPC.RAL.PR.02-024
Issue: 1.0
Date: 30/11/2017
Page: 8

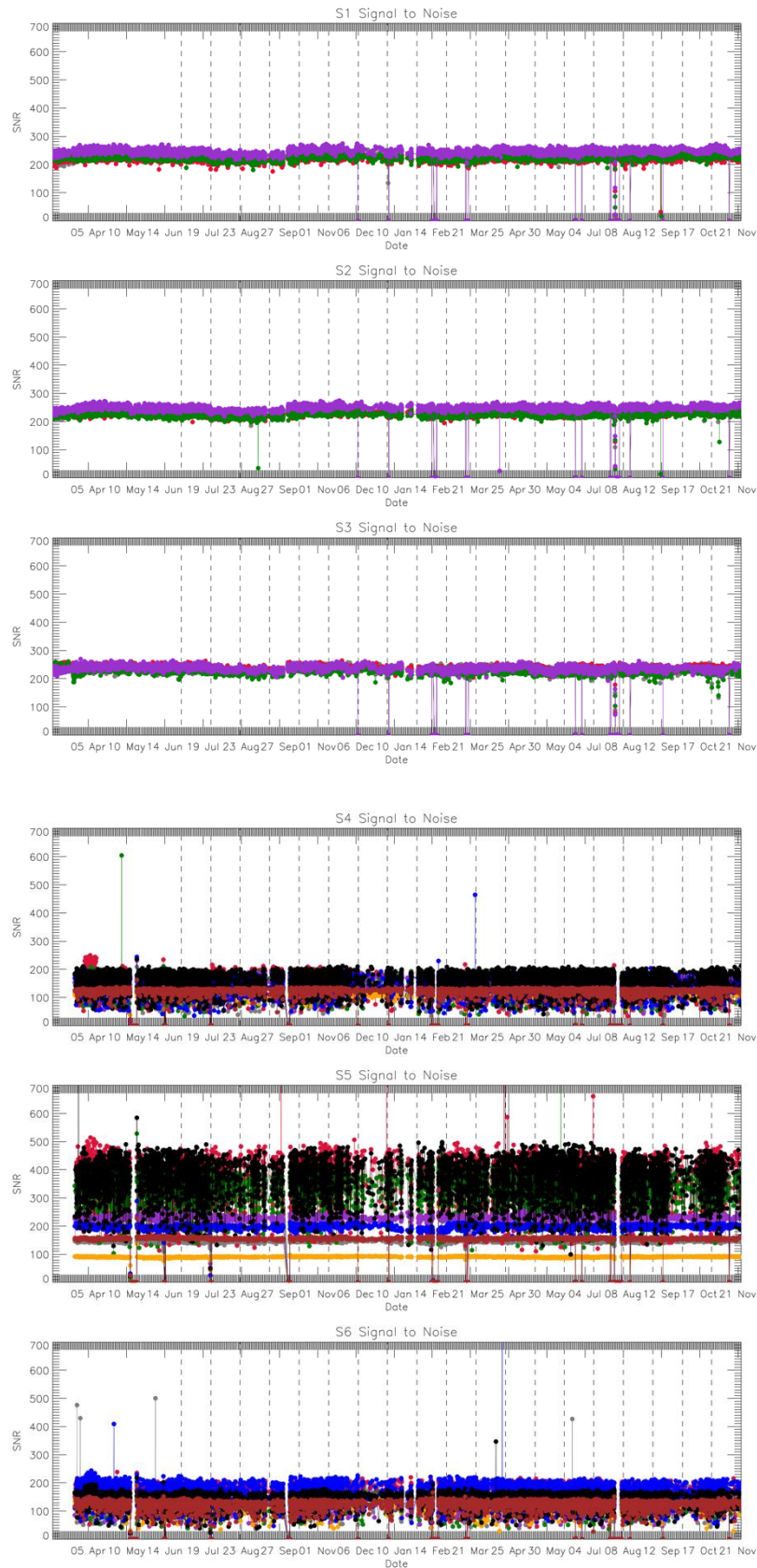


Figure 7: VIS and SWIR channel signal-to-noise of the measured VISCAL signal in each orbit. Different colours indicate different detectors.



Sentinel-3 MPC

S3-A SLSTR Cyclic Performance Report

Cycle No. 024

Ref.: S3MPC.RAL.PR.02-024
Issue: 1.0
Date: 30/11/2017
Page: 9

1.3.2 TIR channel NEDT

The thermal channel NEDT values are consistent with previous operations and within the requirements. NEDT values for each cycle, averaged over all detectors and both Earth views, are shown in Table 3 and Table 4.

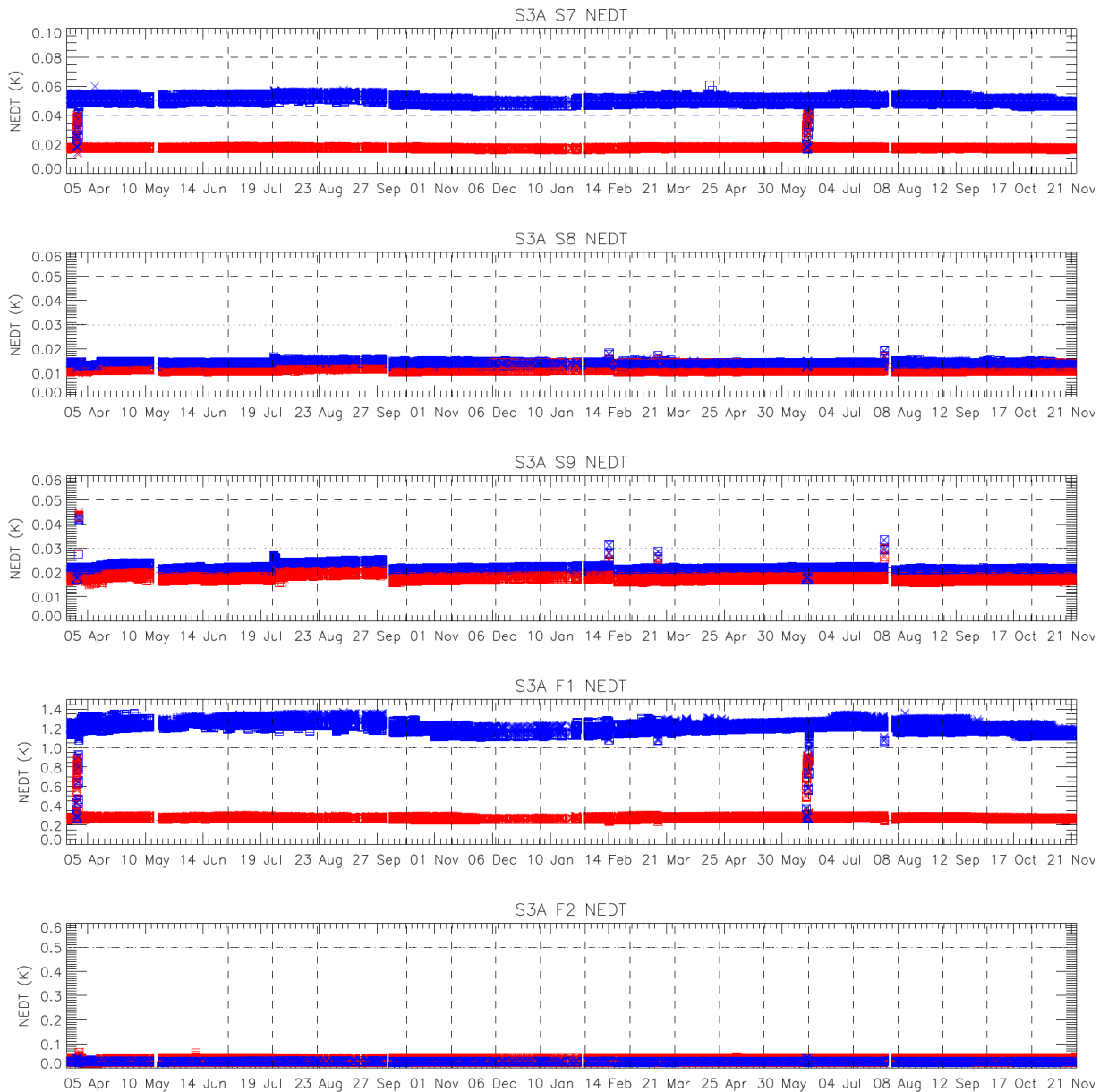


Figure 8: NEDT trend for the thermal channels. Blue points were calculated from the cold blackbody signal and red points from the hot blackbody. Horizontal lines indicate the requirement (dashed) and goal (dotted) as well as the measured values on ground (red and blue dashed).



Sentinel-3 MPC

S3-A SLSTR Cyclic Performance Report

Cycle No. 024

Ref.: S3MPC.RAL.PR.02-024
 Issue: 1.0
 Date: 30/11/2017
 Page: 10

Table 3: NEDT for cycles 013-024 averaged over all detectors for both Earth views towards the +YBB (hot).

	Cycle 013	Cycle 014	Cycle 015	Cycle 016	Cycle 017	Cycle 018	Cycle 019	Cycle 020	Cycle 021	Cycle 022	Cycle 023	Cycle 024
+YBB temp (K)	303.621	303.206	302.674	302.544	302.541	302.593	302.385	302.395	302.316	302.466	303.125	303.406
NEDT (mK)												
S7	16.9	16.8	16.9	17.2	17.2	18.1	17.2	17.2	17.1	17.2	16.9	16.8
S8	11.0	11.1	11.0	10.9	11.0	11.1	11.0	11.1	10.9	10.9	10.9	10.8
S9	17.7	17.9	17.6	17.0	17.2	17.5	17.4	17.5	16.7	16.9	17.0	17.1
F1	260	260	260	268	271	297	276	276	269	270	265	265
F2	28.0	28.0	27.9	27.6	27.8	27.8	27.8	27.8	27.4	27.6	27.7	27.9

Table 4: NEDT for cycles 013-024 averaged over all detectors for both Earth views towards the -YBB (cold).

	Cycle 013	Cycle 014	Cycle 015	Cycle 016	Cycle 017	Cycle 018	Cycle 019	Cycle 020	Cycle 021	Cycle 022	Cycle 023	Cycle 024
-YBB temp (K)	266.353	265.807	265.183	265.136	265.260	265.412	265.122	265.054	264.900	265.012	265.790	266.119
NEDT (mK)												
S7	46.8	47.9	48.7	49.0	48.8	46.9	49.2	49.4	49.4	49.0	47.6	47.2
S8	14.4	14.4	14.2	14.2	14.3	14.2	14.3	14.4	14.2	14.1	14.2	14.1
S9	22.4	22.1	21.3	21.4	21.6	21.6	22.0	22.0	21.1	21.3	21.4	21.4
F1	1130	1178	1222	1191	1199	1163	1231	1233	1212	1202	1161	1144
F2	29.6	29.6	29.2	29.3	29.3	29.4	29.6	29.7	29.2	29.2	29.3	29.3

Note that there may be very small differences in the average NEDT values in Table 3 and Table 4 for recent cycles compared to previous Cyclic Reports because additional products may have been received from the MPC since those reports were published.



1.4 Calibration factors

1.4.1 VIS and SWIR VISCAL signal response

Signals from the VISCAL source for the VIS channels show oscillations due to the build up of ice on the optical path within the FPA. Decontamination must be carried out periodically in order to warm up the FPA and remove the ice. The latest decontamination cycle was successfully performed at the end of Cycle 20. The VISCAL signal has behaved as expected following the decontamination.

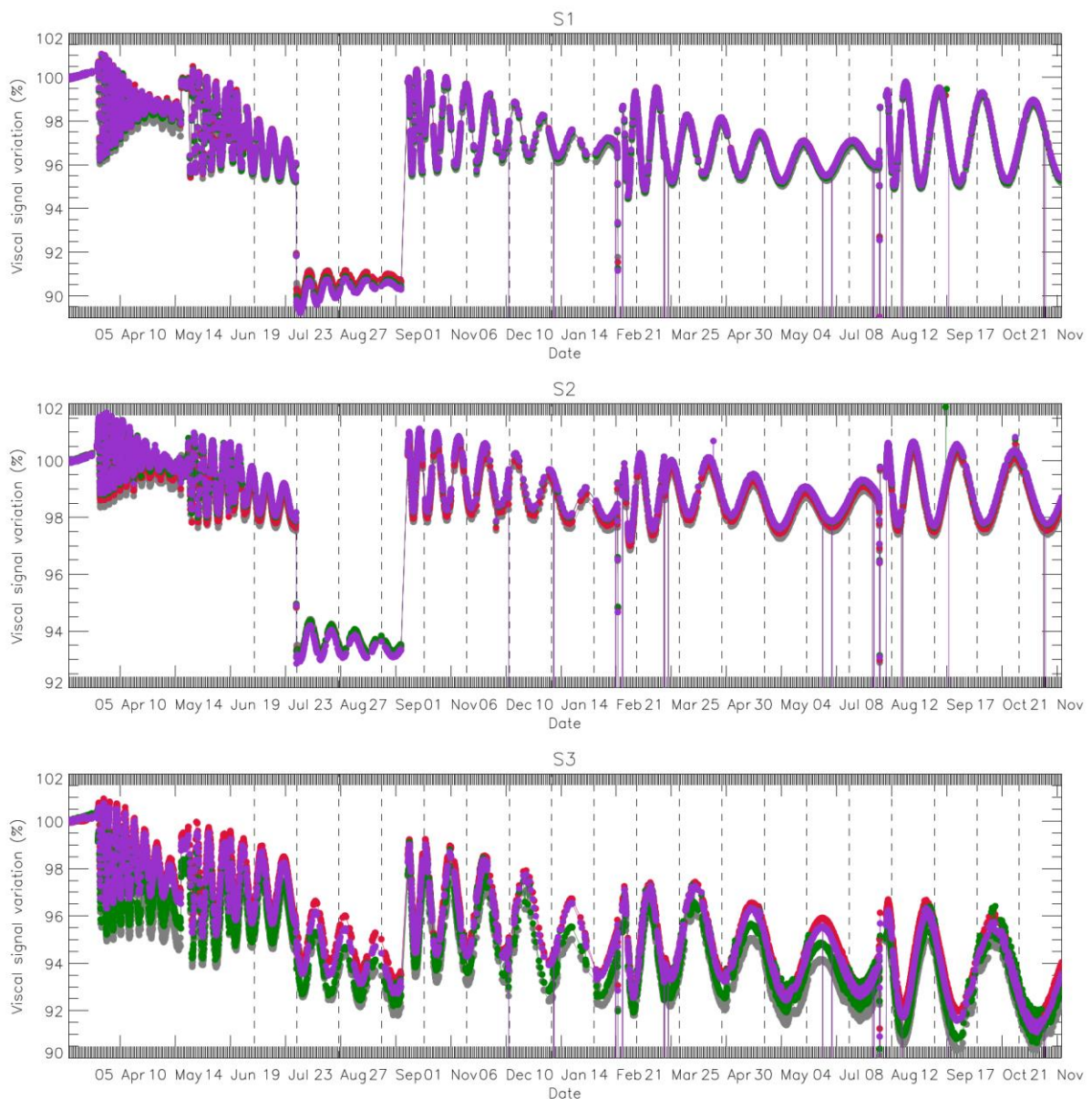


Figure 9: VISCAL signal trend for VIS channels (nadir view).



Sentinel-3 MPC
S3-A SLSTR Cyclic Performance Report
Cycle No. 024

Ref.: S3MPC.RAL.PR.02-024
Issue: 1.0
Date: 30/11/2017
Page: 12

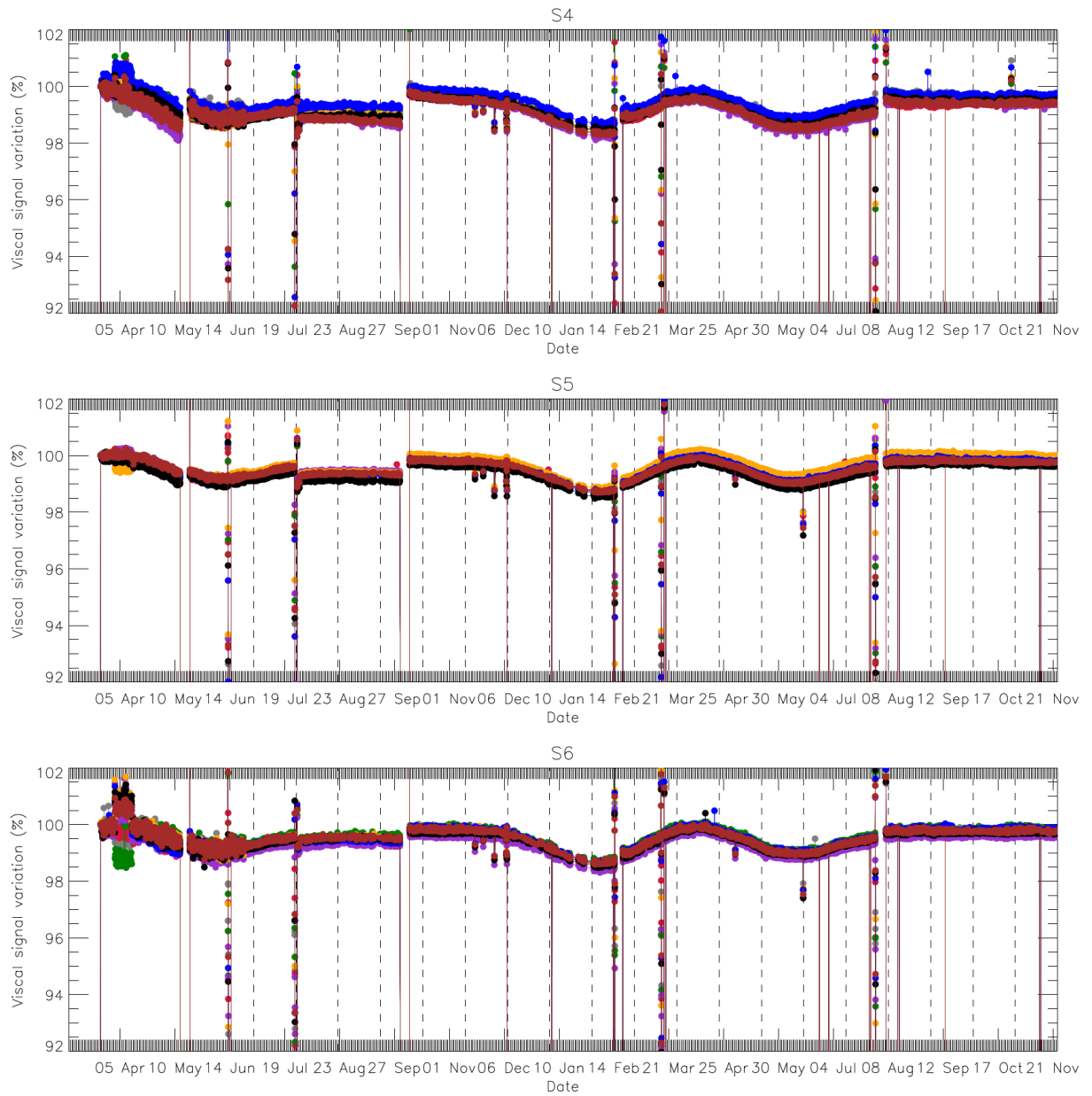


Figure 10: VISCAL signal trend for SWIR channels (nadir view).



2 Level-1 product validation

2.1 Geometric calibration/validation

Regular monitoring using the GeoCal Tool implemented at the MPC is being carried out. This monitors the geolocation performance in Level-1 images by correlation with ground control point (GCP) imageries. Each Level-1 granule typically contains several hundred GCPs, which are filtered based on signal-to-noise to obtain a daily average in the across and along track directions. The results are plotted in Figure 11 up to the 28th October 2017, giving the average positional offsets in kilometres for Nadir and Oblique views. A comparison of Nadir and Oblique results shows that the offset difference between views has been gradually decreasing since July. This will be carefully monitored to determine whether it is due to a seasonal drift or another effect.

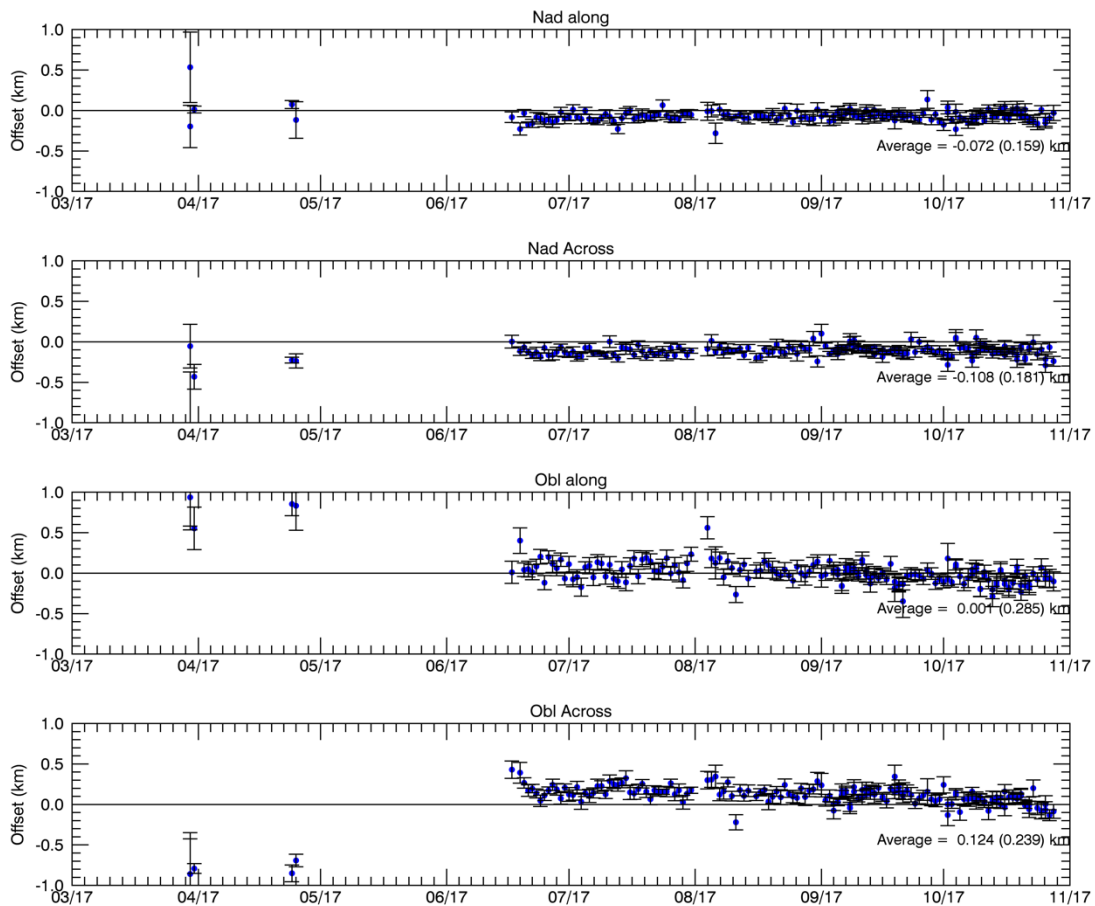


Figure 11: Daily offset results in km from the GeoCal Tool analysis for Nadir along and across track (top two plots) and Oblique along and across track (bottom two plots). The error bars show the standard deviation. The x-axis shows the date (month/year).



2.2 Radiometric validation

The radiometric calibration of the visible and SWIR channels is monitored using the S3ETRAC service. The S3ETRAC service extracts OLCI and SLSTR Level-1 data and computes associated statistics over 49 sites corresponding to different surface types (desert, snow, ocean maximising Rayleigh signal, and ocean maximising sunglint scattering). These S3ETRAC products are used for the assessment and monitoring of the VIS and SWIR radiometry by the ESL.

Details of the S3ETRAC/SLSTR statistics are provided on the S3ETRAC website <http://s3etrac.acri.fr/index.php?action=generalstatistics#pageSLSTR>

- ❖ Number of SLSTR products processed by the S3ETRAC service
- ❖ Statistics per type of target (DESERT, SNOW, RAYLEIGH, SUNGLINT)
- ❖ Statistics per site
- ❖ Statistics on the number of records

Analysis of S3ETRAC results for SLSTR radiometric validation is ongoing and will be presented in future cyclic reports.

2.3 Image quality

The Level-1 image quality is assessed when data are available at the MPC. For example by combining all granules over one day into a single Level-3 image. Figure 12 shows an example Level-3 image for the visible channels from 2nd November 2017 (daytime only). Some problems with images on the 14th November 2017 are described in Section 5.

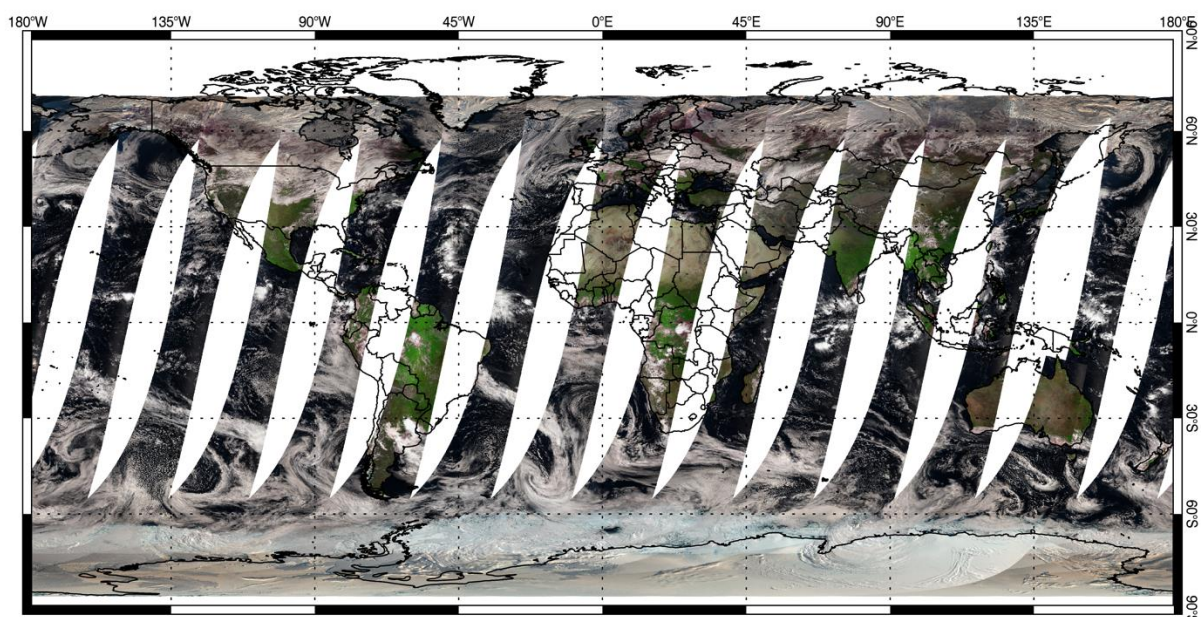


Figure 12: Daytime Level-3 image for visible channels on 2nd November 2017.



3 Level 2 SST validation

Level 2 WCT SSTs have been validated using CMEMS *in situ* data for Cycle 24. Match-ups between SLSTR and *in situ* data are provided by the EUMESAT OSI-SAF.

3.1 Dependence on latitude, TCWV, Satellite ZA and date

- ❖ The dependence of the difference between SLSTR SST_{skin} and drifting buoy SST_{depth} for Cycle 24 is shown in Figure 13. No adjustments have been made for difference in depth or time between the satellite and *in situ* measurements. SLSTR SSTs are extracted from the SL_2_WCT files. Daytime 2-channel (S8 and S9) results are shown in red, night time 2-channel results are shown in blue and night time 3-channel results are shown in green. Solid lines indicate dual-view retrievals, dashed lines indicate nadir-only retrievals. Bold lines indicate statistically significant (95% confidence) results.

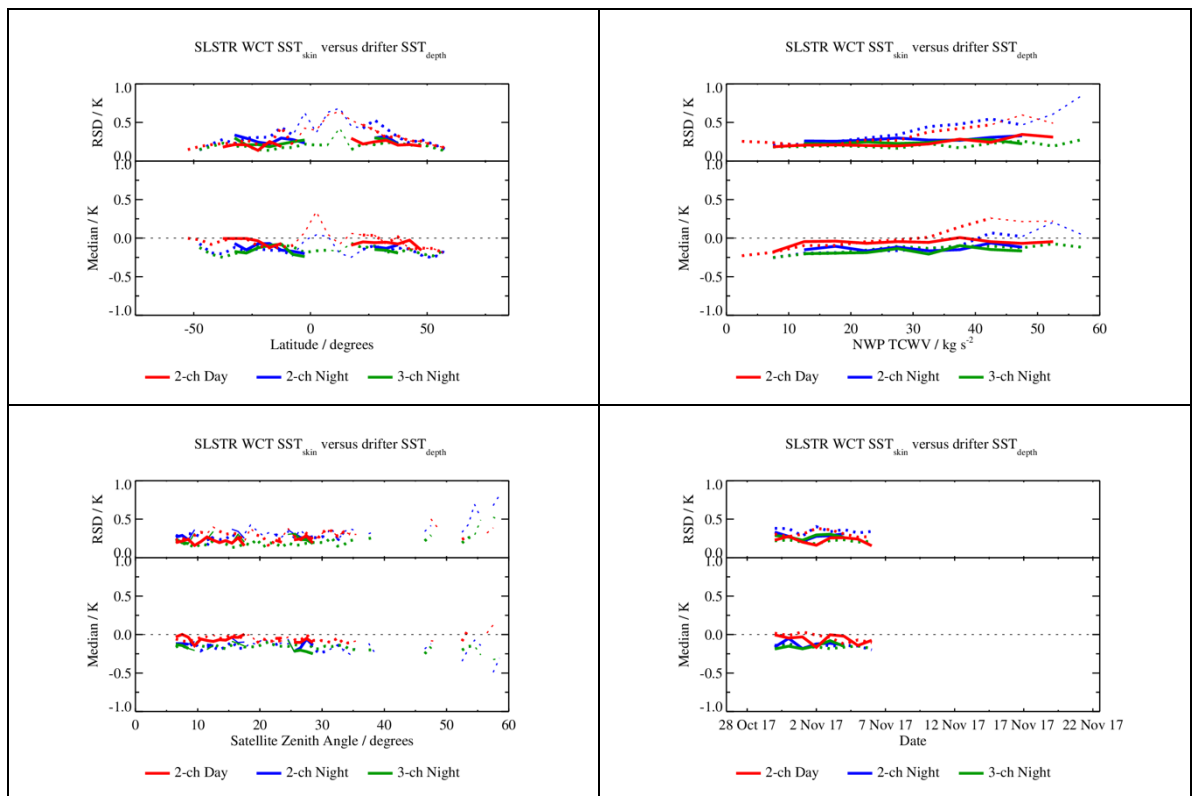


Figure 13: Dependence of median and robust standard deviation of match-ups between SLSTR SST_{skin} and drifting buoy SST_{depth} for Cycle 24 as a function of latitude, total column water vapour (TCWV), satellite zenith angle and date. The data gap towards the end of the cycle is due to a delay in match-up production.



3.2 Spatial distribution of match-ups

- ❖ The spatial distribution of SLSTR/drifter match-ups for Cycle 24 is shown in Figure 14. No adjustments have been made for difference in depth or time between the satellite and *in situ* measurements.

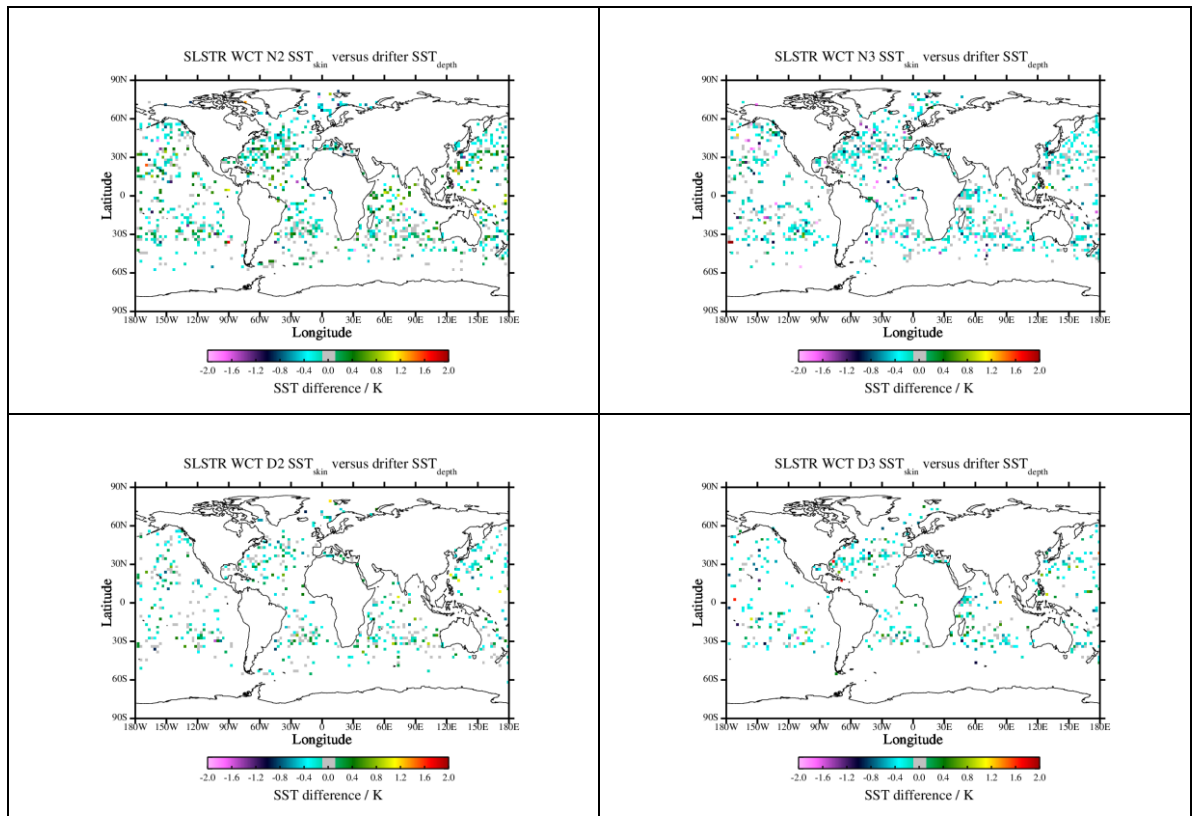


Figure 14: Spatial distribution of match-ups between SLSTR SST_{skin} and drifting buoy SST_{depth} for Cycle 24.



3.3 Match-ups statistics

- ❖ Match-ups statistics (median and robust standard deviation, RSD) of SLSTR/drifter match-ups for Cycle 24 is shown in Table 5. No adjustments have been made for difference in depth or time between the satellite and *in situ* measurements and so at night time (in the absence of diurnal warming) an offset of around -0.17 K is expected. The RSD values indicate SLSTR is providing SSTs mostly within its target accuracy (0.3 K).

Table 5: SLSTR drifter match-up statistics for Cycle 24.

Retrieval	Number	Median (K)	RSD (K)
N2 day	2340	-0.04	0.30
D2 day	1037	-0.06	0.22
N2 night	2367	-0.16	0.34
N3 night	2367	-0.16	0.21
D2 night	889	-0.13	0.28
D3 night	889	-0.17	0.24



4 Level 2 LST validation

Level 2 Land Surface Temperature products have been validated against *in situ* observations (Category-A validation), and intercompared (Category-C validation) with respect to three independent reference products from the ESA DUE GlobTemperature Project (MODIS, GOES, and SEVIRI).

4.1 Category-A validation

Category-A validation uses a comparison of satellite-retrieved LST with *in situ* measurements collected from radiometers sited at a number of stations spread across the Earth, for which the highest-quality validation can be achieved. The results can be summarised as follows (see Figure 15 and Figure 16):

- ❖ Average absolute accuracy (vs. Gold Standard):
 - Daytime: 0.81K
 - Night-time: 1.07K

This daytime accuracy meets the mission requirement of < 1K. The night-time accuracy is very close to this mission requirement. This also is in line with the GCOS climate requirements of 1 K accuracy.

- ❖ Average precision (vs. Gold Standard):
 - Daytime: 0.72K
 - Night-time: 1.21K

While there is no Sentinel-3 mission requirement for precision, the daytime precision meets the GCOS climate requirement of 1K. The night-time accuracy is also very close to this climate requirement.

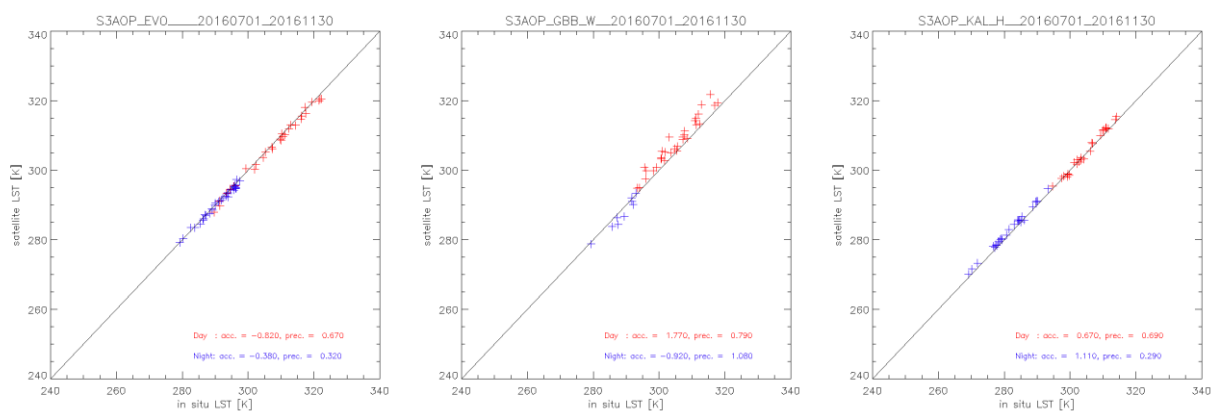


Figure 15: Validation of the SL_2_LST product over the mid-July to mid-November reprocessed period at three Gold Standard in situ stations managed by the Karlsruhe Institute of Technology: Evora, Portugal (left); Gobabeb, Namibia (centre); Kalahari-Heimat, Namibia (right). [Results courtesy of Maria Martin through the GlobTemperature Project]

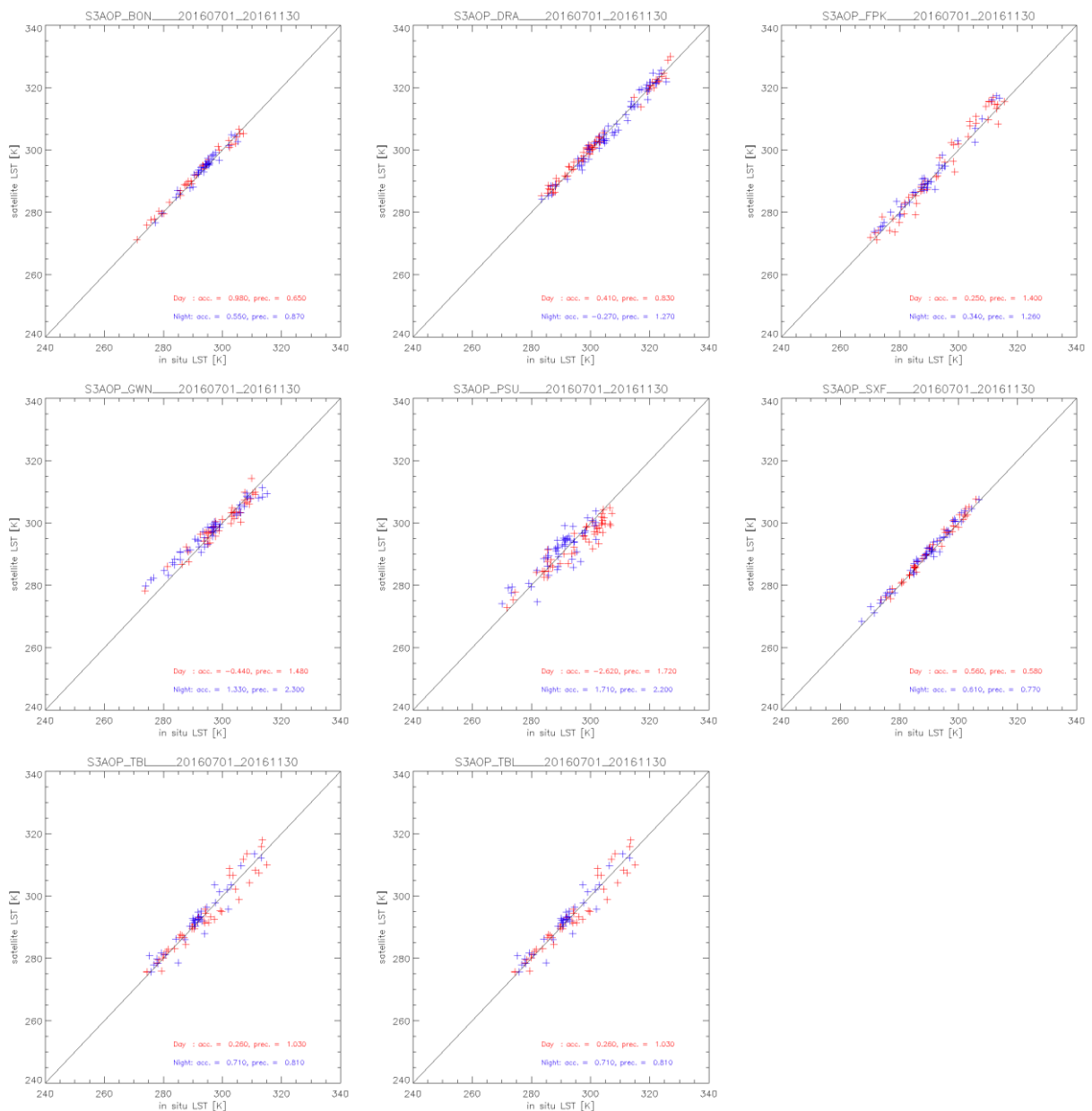



Figure 16: Validation of the SL₂LST product over the mid-July to mid-November reprocessed period at the seven Gold Standard in situ stations of the SURFRAD network plus a Gold Standard station from the ARM network: Bondville, Illinois top-(left); Desert Rock, Nevada (top-centre); Fort Peck, Montana (top-right); Goodwin Creek, Mississippi (middle-left); Penn State University, Pennsylvania (middle-centre); Sioux Fall, South Dakota (middle-right); Table Mountain, Colorado (bottom-left); and Southern Great Plains, Oklahoma (bottom-centre).

	<p>Sentinel-3 MPC</p> <p>S3-A SLSTR Cyclic Performance Report</p> <p>Cycle No. 024</p>	<p>Ref.: S3MPC.RAL.PR.02-024</p> <p>Issue: 1.0</p> <p>Date: 30/11/2017</p> <p>Page: 20</p>
--	---	--

4.2 Category-C validation

Category-C validation uses inter-comparisons with similar LST products from other sources such as AATSR, AVHRR, MODIS, SEVIRI, and VIIRS, which give important quality information with respect to spatial patterns in LST deviations. The results can be summarised as follows:

- ❖ Daytime intercomparison differences are: ~1K vs. GOES__LST_2 over North America; ~1K vs. SEVIR_LST_2 over Europe; and < 1K vs. MOGSV_LST_2 on a Global basis.
- ❖ Night-time intercomparison differences are: <1K vs. GOES__LST_2 over North America; <1K vs. SEVIR_LST_2 over Europe; and < 1K vs. MOGSV_LST_2 on a Global basis.
- ❖ Differences with respect to biomes tend to be larger during the day for surfaces with more heterogeneity and/or higher solar insolation. With respect to SLSTR zenith viewing angle differences are larger in the day on the left side of the SLSTR swath in the along-track direction.



5 Events

SLSTR was switched on and operating nominally during the cycle, with SUE scanning and autonomous switching between day and night modes. However, there was a loss of data at the Svalbard receiving station on 14th November 2017 due to an antenna problem. This caused some missing scans in the SLSTR data between 12:05 and 12:49, affecting Level-1 and Level-2 images. The missing scans appear as stripes, or in some cases granules with no data at all. Figure 17 shows some examples of the Level-1 quicklook image for affected granules.

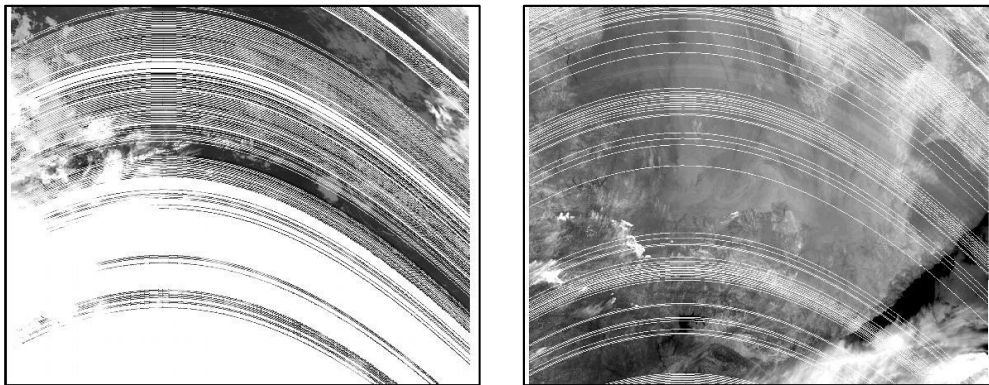



Figure 17: Examples of granules affected by the loss of data on 14th November (12:17-12:20 on the left and 12:40-12:43 on the right).

 The logo for the Sentinel-3 Mission Performance Centre. It features a blue satellite icon at the top, the text 'SENTINEL 3' in blue, and 'Mission Performance Centre' in blue. Below the text are four small square images: a satellite, a landscape, a person, and a globe. A green checkmark is at the bottom right.	<p style="text-align: center;">Sentinel-3 MPC</p> <p style="text-align: center;">S3-A SLSTR Cyclic Performance Report</p> <p style="text-align: center;">Cycle No. 024</p>	<p>Ref.: S3MPC.RAL.PR.02-024</p> <p>Issue: 1.0</p> <p>Date: 30/11/2017</p> <p>Page: 22</p>
---	---	--

6 Appendix A

Other reports related to the Optical mission are:

- ❖ S3-A OLCI Cyclic Performance Report, Cycle No. 024 (ref. S3MPC.ACR.PR.01-024)

All Cyclic Performance Reports are available on MPC pages in Sentinel Online website, at: <https://sentinel.esa.int>

End of document